THE ASTROPHYSICAL JOURNAL, 201:L15–L19, 1975 October 1

THE CRAB NEBULA: HIGH ENERGY X-RAY OBSERVATION OF A LUNAR OCCULTATION

R. STAUBERT, E. KENDZIORRA, AND J. TRÜMPER
Astronomisches Institut der Universität Tübingen

C. REPPIN
Max-Planck-Institut für Extraterrestrische Physik, München

J. A. HOFFMAN, K. A. POUNDS, AND A. B. GILES
University of Leicester, Leicester

AND

L. V. MORRISON
H.M. Nautical Almanac Office, Royal Greenwich Observatory, Herstmonceux
Received 1975 March 28; revised 1975 July 15

ABSTRACT

A lunar occultation of the Crab Nebula was observed at X-ray energies above 15 keV by a scintillation counter on a Skylark rocket launched from Spain on 1974 October 7. The angular extent of the region of emission of 75 percent of the total flux between 15 and 150 keV (average photon energy 39 keV) along position angle 263° is found to be 110″ ± 25″. The offset of the centroid of the extended source is such that its projection to the west of NP 0532 is 8″ ± 6″. The variation of size with energy, as found from this and other measurements, sets constraints on models for energy transfer along magnetic field lines in the Crab.

Subject headings: Crab Nebula — X-ray sources

I. INTRODUCTION

The current cycle of lunar occultations of the Crab Nebula has provided a unique opportunity to study the spatial distribution of the Crab's X-ray emission. We report here the results of a joint British-German rocket experiment to observe the 1974 October 7 occultation visible over the North Atlantic and Europe.

II. OBSERVATIONS

A Skylark rocket carrying proportional and scintillation counters was launched from the Spanish test range, El Arenosillo, at $06^h33^m30^s$ UT on 1974 October 7. It reached an apogee of 190 km and provided 240 s observing time above 100 km. The lunar limb cut the Crab along position angle 263°. The position of the rocket was measured to ±500 m during flight using radar transponder data, which enabled the position of the lunar limb as seen from the rocket to be calculated to ±0″.3, the main uncertainty being the intrinsic position of the Moon. Shortly before launch, the proportional-counter power supply failed, so data are available only from the scintillation counter.

The scintillation counter was an assembly of four 10 × 10 × 0.5 cm CsI(Na) crystals, each embedded in 4 mm of plastic scintillator, viewed by an EMI 9514 phototube and covered by a steel plate collimator. A pointing offset during the flight, combined with loss of data from one unit due to excessive noise, left a total effective area of 155 cm^2 viewing the Crab. The low-energy threshold of the system was 15 keV. ^{241}Am sources were rotated in front of the detectors at the beginning and end of the flight for calibration.

Figure 1 shows the observed count rates for the three remaining detector units plotted against the angular separation of the lunar limb and the Crab pulsar. The occultation is clearly visible. About 12 s of background data are available before the Crab was acquired in the field of view, agreeing well with the background

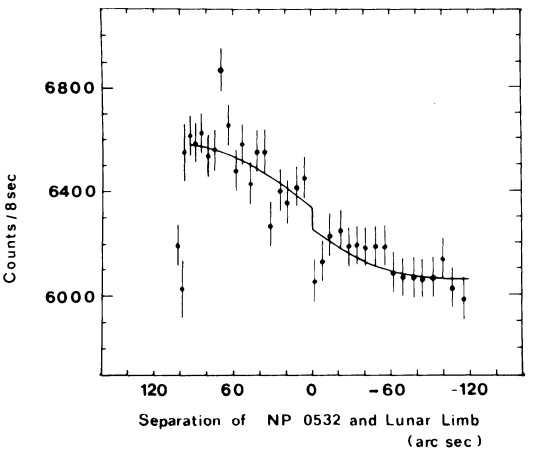

FIG. 1.—Counting rate data for the high-energy X-ray observation of the lunar occultation of the Crab on 1974 October 7. The time for the individual integration periods of 8 s has been converted into the actual angular separation of the lunar limb and the pulsar NP 0532 using the measured rocket trajectory. Error bars shown on individual data points are ±1 σ and are purely statistical. The solid line is the minimum χ^2 fit assuming an extended source with a Gaussian emission profile plus a superposed point source with 15% of the total flux.

observed after the occultation. Toward the end of the occultation observation, telemetry noise caused the loss of time resolution for two periods of about 30 s each (−22″ to −51″ and −64″ to −94″ in Fig. 1). The total counts in these periods have been equally divided into four count rate bins each.

The first step in the analysis was to evaluate the pre- and postoccultation count rates. The difference between these rates corresponds to 0.40 ± 0.02 counts cm^{-2}, which was the expected rate from the Crab. In finding the other source parameters these levels have not been varied. One-dimensional strip intensity distributions of the Crab at radio (Wilson 1972*a*) and optical (Woltjer 1957) wavelengths show roughly Gaussian profiles. Measurements of NP 0532 at energies greater than 15 keV (Boclet *et al.* 1972; Laros *et al.* 1973) show a pulsed fraction of ∼15 percent. In fitting the data, we have adopted as the primary model a one-dimensional Gaussian emission profile of variable width and position, together with a delta function at the position of NP 0532 with 15 percent of the total intensity. In order to check for systematic uncertainties connected with the choice of a special source model we also performed fits using a one-dimensional rectangular emission profile and a two-dimensional circular source with constant surface brightness. All models were run as well without a point source and with a variable point-source fraction. Each model was fitted to the data with the minimum chi-squared technique.

Table 1 summarizes the results of the individual fits to the data about which we note the following:

a) All 34 data points after acquisition of the Crab were used for the χ^2 analysis. Fluctuations in all the data are consistent with Poisson statistics; however, the "goodness-of-fit" for a given model is better shown by χ^2_{min} for the 21 data points distributed symmetrically about the diffuse emission centroid, since only these points are sensitive to the model parameters. Table 1 shows the degrees of freedom and χ^2_{min} both for the entire set of data and for the central, model-dependent region. The errors listed in Table 1 correspond to $\chi^2_{min} + 1$.

b) We find the size of the extended source and its offset from the point source quite insensitive to the assumed emission profile and the fractional intensity of the point source.

c) The rectangular and circular profiles give marginally lower χ^2 fits, but the differences are not statistically meaningful.

d) The smallest χ^2 values occur for a point source fraction of 30–32 percent. Our knowledge of the lunar limb position was exact enough to fix the point source position. However, we let it vary as a check and found a χ^2_{min} point-source position within ±2″ of the pulsar position. The large statistical fluctuation on either side of the pulsar position clearly influences this result, as it does the point-source fraction.

For interpretation and comparison with other measurements we derive three characteristic parameters from the best fits for each model: D_{75}, the angular extent of the emission region from which 75 percent of the total flux originates (∼FWHM for a Gaussian profile); d, the separation of the pulsar and the centroid of the extended source, projected along position angle 263°; and I_{west}/I_{east}, the intensity ratio of the part of the nebula in the "west" of the pulsar to that in the "east." The second and third parameters describe in two different ways the same physical facts. When these

TABLE 1

SIZE, OFFSET, AND POINT-SOURCE FRACTION OF THE CRAB NEBULA AS MEASURED BY THE PRESENT EXPERIMENT, DERIVED FOR VARIOUS SOURCE MODELS

EMISSION PROFILE OR SOURCE MODEL	NO. OF FREE PARAMETERS	ALL DATA POINTS		MODEL-DEPENDENT CENTRAL DATA POINTS ONLY		D_{75} [arcsec]	d [arcsec]	I_{west}/I_{east}	POINT-SOURCE FRACTION (%)
		Degrees of freedom	χ^2_{min}	Degrees of freedom	χ^2_{min}				
A. One-dimensional Gaussian profile:									
1. 15% point source	2	32	42.5	19	27.4	110±25	8±6	1.2	
2. No point source	2	32	46.1	19	31.0	107±26	8±5	1.2	
3. Free point-source fraction	3	31	41.2	18	26.1	118±26	9±27	1.2	31±11
B. Rectangular profile (single slope):									
1. 15% point source	2	32	42.3	19	27.2	100±15	5±5	1.1	
2. No point source	2	32	45.7	19	30.6	99±13	3±3	1.1	
3. Free point-source fraction	3	31	40.2	18	25.1	113±14	6±26	1.2	30±4
C. Uniform circular source:									
1. 15% point source	2	32	42.2	19	27.1	107±20	6±6	1.2	
2. No point source	2	32	46.6	19	31.5	99±23	6±5	1.2	
3. Free point-source fraction	3	31	40.5	18	25.4	107±14	7±27	1.2	32±10

parameters are used to compare different observations the scan directions of the actual occultations must always be considered.

The results of this experiment are best represented by these characteristic parameters for our primary model (Gaussian, 15% point source): $D_{75} = 110'' \pm 25''$, $d = 8'' \pm 6''$, and $I_{west}/I_{east} = 1.2 \pm 0.1$. The occultation curve corresponding to this model is superposed on the data in Figure 1.

III. DISCUSSION

Table 2 summarizes measurements concerning the fraction of the total X-rays coming from a point source at the pulsar position, the magnitude and direction of any offset of the extended emission from NP 0532, and the X-ray size (and the variation in size with X-ray energy) of the Crab nebula.

a) Point Source Fraction

Our best fit value of 31 ± 11 percent agrees with the average best fit value of 31 ± 9 percent for the two occultation scans observed at energies >20 keV by Ricker *et al.* (1975). The recent occultation observation at energies >20 keV by Fukoda *et al.* (1975) yields a fraction of 26.5 percent (no error given). These occultation results may all indicate (1) a pulsed fraction higher than previously reported or (2) a nonpulsed point-source component. The observation of a large point-source fraction along several scan directions rules out its being caused by a line source of X-rays. For the highest temperatures compatible with the fact that Bowyer *et al.* (1964) did not see a point source in the 1964 Crab occultation, there can be no observable thermal radiation from the surface of the neutron star at energies above 15 keV.

b) Offset of Extended Emission from NP 0532

The centroid of optical continuum emission is offset about 15″ to the NW of the pulsar (Woltjer 1957), so the discovery of this offset in X-rays is not completely unexpected. Other features show similar offsets, such as the central contour of the map (Wilson 1972*b*, Fig. 1) showing contours of constant spectral index between radio and optical frequencies and the wisp activity

TABLE 2

MEASUREMENTS OF THE SIZE AND THE POSITION OF THE X-RAY SOURCE IN THE CRAB NEBULA

Reference and Institute	Date	Technique	Assumed Emission Profile and Remarks	Energy (keV)	Offset to Pulsar [arcsec]	Position angle (degrees)	Size [arcsec]
Bowyer *et al.* (1964) (NRL)	1964 July 7	Occultation, proportional counter, rocket	Actual shape derived from data	2–10	≤(2–3) ±5	~310	120
Oda *et al.* (1967) (MIT/ASE)	1966 Mar. 8	Modulation collimator, proportional counter, rocket	Rectangular	1–6	18 NW	~325 ~ 27	110±25 60±60 ~100
Floyd (1970) (MIT)	1969 May 10	Modulation collimator, scintillation counter, balloon	Rectangular, with allowance for a Gaussian	25–100	None	145 222	≥66 ≥66
Hawkins *et al.* (1974) (MSSL)	1973 Jan. 14	Raster scan, grazing incidence telescope, satellite	Uniform disk	1–3.1 0.6–1.8	None None	... ...	66 (+37, −27) 89 (+14, −10)
Ricker *et al.* (1975) (MIT)	1974 Aug. 13	Occultation, scintillation counter, balloon	Gaussian, extent refers to 75% of emission	20–150	10±4 NW	130 244	24± 7 49± 7
Davison *et al.* (1975) (MSSL)	1974 Oct. 7	Occultation, proportional counter, satellite	Rectangular, 100% of emission	1.5–7.5	20±8 W	236 275	73±38 71±15 − 8
This paper (AIT/MPE/UL)	1974 Oct. 7	Occultation scintillation counter, rocket	Rectangular, disk or Gaussian, extent refers to 75% of emission	15–150	8±5 W (projected)	263	110±25
Wolff *et al.* (1974) (CU)	1974 Nov. 3	Occultation, proportional counter, rocket	Extent refers to 80% of emission between W limb and pulsar compact source near the pulsar with continuous emission	1.5–20	?	255	36 (×2)
Palmieri *et al.* (1975) (LRL)	1974 Dec. 28	Occultation, proportional counter, rocket	Little variation with energy, 100% of emission	0.5–16 several intervals	?	278	100

(Scargle 1969*b*). There is no generally accepted reason for this offset, although Aschenbach and Brinkmann (1975) have recently shown how such an offset could result from the observed proper motion of the pulsar with respect to the nebula.

Figure 2 (Plate L1) summarizes the offsets found by various experimenters, superposed on a print of the central region of the Crab Nebula. The $8'' \pm 5''$ offset that we found toward position angle 263° could be the projection of a $13'' \pm 8''$ offset toward p.a. 315°, which is consistent with the MIT result (Ricker *et al.* 1975) of a $10'' \pm 4''$ offset toward the NW of NP 0532. Davison *et al.* (1975) find an emission centroid offset of $20'' \pm 8''$ to the west of NP 0532, i.e., southwest of other observed offsets. This is a result of two intesecting occultations, so there is no freedom to project the offset onto the major axis of the nebula. Although the reason for an offset along the axis of symmetry is not understood, an offset off this axis seems even more difficult to explain. Scargle (1969*a*) finds that although the wisps are offset from the pulsar along the NW–SE axis and exhibit (especially wisp 1) considerable motion along this axis, the offset and motion along the NE–SW axis (parallel to the magnetic field) is less than a few arcsec.

c) Size of X-ray Emission Region

Models of energy transfer in the Crab by MHD waves (Barnes and Scargle 1973) or by electron diffusion (Wilson 1972*b*) predict a large asymmetry between transfer along and across the magnetic field lines. The magnetic field near the center of the nebula runs NE–SW (Walraven 1957; Wilson 1972*a*, *b*). Ricker *et al.* (1975) report that at energies above 20 keV the X-ray emission region in the NE–SW direction (minor axis of the nebula) is twice as large as in the NW–SE direction (major axis). As the present experiment measured the size of the nebula only at p.a. 263°, we only discuss the size and energy dependence of the size of the nebula in directions between E–W (p.a. 270°) and NE–SW (p.a. 225°), i.e., roughly along the direction of the central magnetic field.

At position angle 263°, our measured size of $110'' \pm 25''$ is twice as large as the MIT result of $49'' \pm 7''$ at p.a. 244°. The only other size measurement along this direction at energies above 20 keV is by Floyd (1970), who saw no modulations when scanning the Crab with a modulation collimator/scintillation counter, implying a size greater than 66″ along p.a. 222°. When Ricker *et al.* (1975) allowed the point-source fraction to vary instead of fixing it at 15 percent, the "measured" size became $61'' \pm 9''$. The size we measure is less sensitive to the point-source fraction (see Table 1). Counting statistics of the two experiments are similar. Our fixed-fraction size is larger than MIT's by 2.2 σ whereas the variable fraction results differ by 1.9 σ. This means there is $\gtrsim$90 percent probability that the size we measured really is larger than that measured by Ricker *et al.* (1975).

The average X-ray energy observed from the Crab was 35 keV by our rocket experiment and 50 keV by the MIT balloon experiment. Reconciling the results of the two experiments requires a strong energy dependence on the size of the Crab along the NE–SW axis. The 75 percent diameters of the Crab at optical (Oort and Walraven 1975; Woltjer 1957) and radio (Seeger and Westerhout 1957; Wilson 1972*a*) frequencies are about 2′.5 and 3′.5, respectively, along the minor axis. Most X-ray observations below 20 keV (see Table 2) show sizes $\gtrsim$100″, with little dependence of size on energy. The small and smooth size variation from radio to medium energy X-rays does not suggest a drastic decrease in size over the narrow energy range from 35 to 50 keV.

Ricker *et al.* (1975) find a close spatial association between the wisp region and the high-energy X-ray emitting region. The ambient nebular magnetic field is concentrated along the wisps (Scargle 1971), so electrons striking the wisp will radiate at higher energies than in the surrounding medium. X-rays above a given energy are likely to be produced mainly in the wisps and will share the sharp spatial boundaries of the wisp region. The emission region for lower energy X-rays is more diffuse and will show a smaller dependence of size on energy. This may explain the unexpectedly sharp size change between 35 and 50 keV.

We wish to acknowledge the work done by the British Skylark integration team of BAC, the German launch team of the DFVLR-MoRaBa and the authorities of the Spanish rocket range El Arenosillo, who all made the success of this experiment possible. We thank the MIT group for communicating the results of their occultation observations to us in Spain prior to launch. We also thank E. Nagel of the TU München and E. Thürring, MPE, for performing postobservation calculations on the occultation as it was seen by the detectors during the actual flight. The work was supported by the British Science Research Council (SRC) and the German Bundesministerium für Forschung und Technologie (BMFT).

REFERENCES

Aschenbach, B., and Brinkmann, W. 1975, submitted to *Astr. and Ap.*
Barnes, A., and Scargle, J. 1973, *Ap. J.*, **184**, 251.
Boclet, D., Brucy, G., Claisse, J., Durouchoux, Ph., and Rocchia, R. 1972, *Nature Phys. Sci.*, **235**, 69.
Bowyer, F., Byram, E. T., Chubb, T. A., and Friedman, H. 1964, *Science*, **146**, 912.
Davison, P. J. N., Culhane, J. L., and Morrison, L. V. 1975, *Nature*, **253**, 610.
Floyd, F. W. 1970, *Nature*, **226**, 733.
Fukoda, Y., Hayakawa, S., Kasahara, I., Makino, F., Tanaka, Y., Akiyama, H., Matsuoka, M., Nishimura, J., Oda, M., Nakagawa, M., Sakurai, H., Iyengar, V. S., Kunte, P. K., Manchauda, R. K., and Sreekantan, B. V. 1975, *Nature*, **255**, 465.
Hawkins, F. J., Mason, K. O., Sanford, P. W., and Culhane, J. L. 1974, *M.N.R.A.S.*, **169**, 41.
Laros, J. G., Matteson, J. L., and Pelling, R. M. 1973, *Nature Phys. Sci.*, **246**, 109.

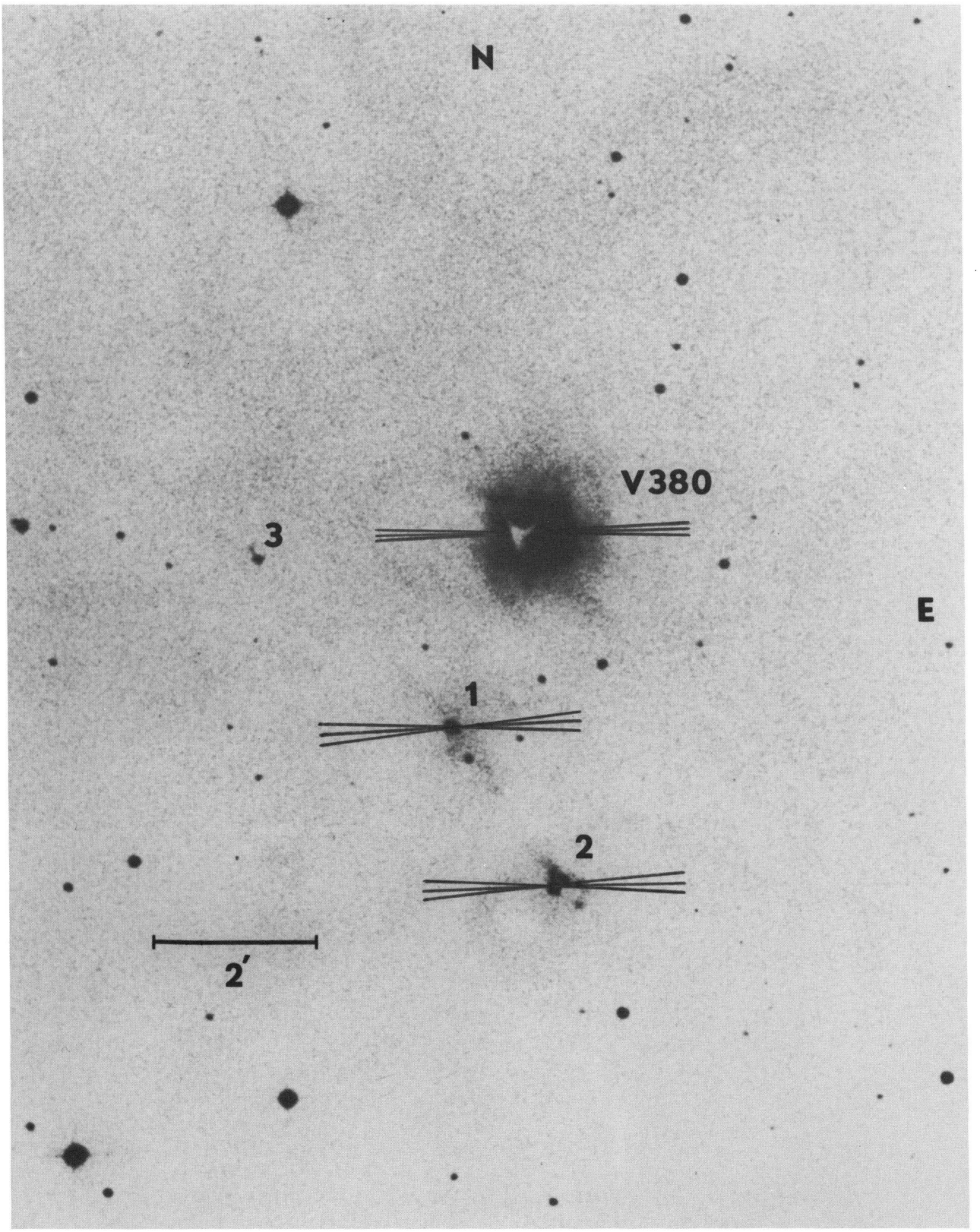

FIG. 2.—Central region of the Crab Nebula, showing NP 0532 and the wisp region. Superposed on this are the locations of the centroid of X-ray emission determined by the MIT group (Ricker *et al.* 1975), the MSSL group (Davison *et al.* 1975) and the present AIT/MPE/LU experiment. The two former results are the intersections of two scans and give actual locations with $\pm 1\ \sigma$ errors shown for each scan direction. The present single-scan result gives only a line of position, with the dotted lines to either side showing the $\pm 1\ \sigma$ errors. The centroid of optical emission lies about 18″ NW of NP0532. The photograph is by J. Scargle, 1968 October 23/24, 103aD + 0G1, 20 minute exposure, seeing 3.

STAUBERT *et al.* (*see* page L18)

Oda, M., Bradt, H., Garmire, G., Spada, G., Sreekantan, B. V., Gursky, H., Giacconi, R., Gorenstein, P., and Waters, J. R. 1967, *Ap. J.* (*Letters*), **148**, L5.
Oort, J. H., and Walraven, Th. 1956, *B.A.N.*, **12**, 285.
Palmieri, T. 1975, private communication.
Palmieri, T., *et al.* 1975, preprint.
Ricker, G. R., Scheepmaker, A., Ryckman, S. G., Ballintine, J. E., Doty, J. P., Downey, P. M., and Lewin, W. H. G. 1975, *Ap. J.* (*Letters*), **197**, L83.
Scargle, J. D. 1969*a*, *Ap. Letters*, **3**, 73.
———. 1969*b*, *Ap. J.*, **256**, 401.
———. 1971, *Nature Phys. Sci.*, **230**, 37.
Seeger, C. L., and Westerhout, G. 1957, *B.A.N.*, **13**, 312.
Walraven, Th. 1957, *B.A.N.*, **13**, 293.
Wilson, A. S. 1972*a*, *M.N.R.A.S.*, **157**, 229.
———. 1972*b*, *ibid.*, **160**, 355.
Wolff, R. S., Kestenbaum, H., Ku, W., and Novick, R. 1974, *IAU Circ.*, No. 2731.
Woltjer, L. 1957, *B.A.N.*, **13**, 301.

A. B. Giles and K. A. Pounds: Physics Department, University of Leicester, Leicester LE1 7RH, England

J. A. Hoffman: Center for Space Research, 37-601, Massachusetts Institute of Technology, Cambridge, MA 02139

L. V. Morrison: Royal Greenwich Observatory, Herstmonceux Castle, Hailsham, Sussex, England

R. Staubert and E. Kendziorra: Astronomisches Institut der Universität Tübingen, 74 Tübingen, Germany

J. Trümper and C. Reppin: Max-Planck-Institut für Extraterrestrische Physik, 8046 Garching b. München, Germany